INSTITUTE OF PHYSICS PUBLISHING JOURNAL OF PHYSICS: CONDENSED MATTER

J. Phys.: Condens. Matter **18** (2006) S2527–S2542 doi:10.1088/0953-8984/18/38/S01

Nanocrystalline iron oxide and Ba ferrite particles in the superparamagnetism–ferromagnetism transition range with ferrofluid applications

Robert Müller, Rudolf Hergt, Silvio Dutz, Matthias Zeisberger and Wolfgang Gawalek

Institut für Physikalische Hochtechnologie, POB 100239, D-07702 Jena, Germany

E-mail: robert.mueller@ipht-jena.de

Received 1 May 2006, in final form 5 July 2006
Published 8 September 2006
Online at stacks.iop.org/JPhysCM/18/S2527

Abstract

Magnetic fluids based on Ba hexaferrite as well as iron oxide particles with enhanced anisotropy barriers show heating effects in ac magnetic fields which may be useful in technical processes as well as medical applications (magnetic hyperthermia). Such particles also allow the detection of biological binding reactions through an enhanced Néel relaxation time above the Brown relaxation. The loss processes and the relaxation times depend strongly on the mean particle size and the size distribution width. To influence and improve the mean size as well as the size distribution, new approaches to the preparation are promising, where nucleation and growth of the particles can be influenced independently or where further growth is possible on small given particles without further nucleation. We used a glass crystallization method for preparation of nanocrystalline Ba hexaferrite as well as magnetic iron oxide and a cyclic growth method based on 'conventional' precipitation for iron oxide preparation. Properties of the powders prepared, as well as water based ferrofluids, were analysed using x-ray diffraction, transmission electron microscopy and magnetic methods. Values of the specific loss power of the order of 100 W/g maghemite may be achieved with the option of further increase by improving the core size distribution.

1. Introduction

Usual commercial ferrofluids consist of nanoparticles (mostly iron oxide) of the order of 10 nm in size which behave superparamagnetically. However for certain applications a stable particle suspension with enhanced hysteretic remagnetization losses or a slow decrease of the remanent magnetization (enhanced Néel relaxation time) is desired. These properties can be obtained by means of an increased anisotropy barrier, i.e. a bigger (mean) size of the iron oxide particles or a higher effective anisotropy constant, using materials like Ba ferrite. In contrast to the case

for such samples, in the superparamagnetism–ferromagnetism transition range the preparation of stable fluids from particle ensembles with pure ferromagnetic/ferrimagnetic behaviour is difficult or even impossible because of increased agglomeration and sedimentation. High losses and suitable relaxation times may be useful for technical heating processes or for application in magnetic particle hyperthermia proposed as a tumour therapy in ac fields and allow the detection of biological binding reactions, respectively.

For a given material (i.e. one with magnetocrystalline anisotropy) several types of loss which may appear during remagnetization of magnetic nanoparticles (hysteresis losses, Néel or Brown relaxation) depend strongly on the mean particle size (Hergt *et al* 2002), the size distribution width (Hergt *et al* 2004a, 2004b) and the field parameters (see also Hergt *et al* 2006). There is an overlap of the critical size regions of Néel relaxation and hysteresis losses at about 20 nm for magnetite (Hergt *et al* 1998) which should be shifted to smaller diameters for materials with higher crystal anisotropy. To influence and improve the size distribution of magnetic particles new approaches to the preparation are promising, where nucleation and growth of the particles can be influenced independently, like in the process of crystallization of glass or where a further growth is possible on small given particles without further nucleation. The second approach was demonstrated for a non-aqueous system by Klokkenburg *et al* (2004).

Barium hexaferrite $BaFe_{12-2x}Ti_xCo_xO_{19}$ with $x \leqslant 0.8$ has an intrinsic anisotropy one order higher than that of magnetite. Néel relaxation is mainly defined by the size distribution of the particles. The influence of shape anisotropy is weak for magnetically uniaxial particles but may play a role for particles with planar anisotropy. The remanent magnetization of doped barium hexaferrite which is interesting as regards magnetic markers for DNA detection in a biochip based on a magnetoresistive sensor (Brückl *et al* 2004) or for technical heating applications was investigated.

Iron oxide (magnetite or maghemite) is the only ferromagnetic/ferrimagnetic material in powder form suitable for medical applications. In hyperthermia an enhancement of the specific loss power (SLP) of magnetic ac losses at lower field amplitudes would allow a reduction of the tissue load with magnetic material and improve the reliability of a therapy. It is required as well for new kinds of administration of particles like in antibody targeting. Magnetic fluids with suitable particles of about 20 nm are not commercially available. Therefore investigations on the preparation of magnetic fluids based on iron oxide from both methods, glass crystallization and cyclic precipitation, were carried out.

2. Nanocrystalline Ba ferrite particles

2.1. Preparation by glass crystallization

Barium hexaferrite $BaFe_{12-2x}Me^{2+}_xMe^{4+}_xO_{19}$ particles (M-type hexaferrite) were prepared by a glass crystallization method. The method was originally developed for synthesis of single-domain barium hexaferrite particles ($BeFe_{12}O_{19}$) (Shirk and Buessem 1970). The formation of the particles in a borate matrix is a complex process (Görnert *et al* 1991). The method (particle formation during a temperature treatment in a glass matrix and subsequent dissolving of the matrix) allows the preparation of oxide powders of good phase purity. Substitution elements for adjusting intrinsic magnetic properties can be added homogeneously in the melt state. The particles are single crystalline because of their isolated growth in a solid matrix.

To realize a controlled crystallization of particles an amorphous supersaturated initial material is necessary. The glasses are prepared from components of the desired ferrite and additionally B_2O_3 as a glass network former by a rapid cooling (about 10^4 K s^{-1}) by means of the twin-roller technique (after Chen and Miller 1970) fast enough to prevent nucleation

and particle growth. During a temperature treatment of the glass flakes between the glass transformation and melting temperature, phase separation and crystallization of the particles occurs. Phase composition, yield and particle size depend on glass composition and annealing conditions (temperature and time). To obtain the particles the matrix is dissolved using a weak diluted acid, mostly acetic acid. The acidic slurry could be washed and dried.

Replacing Fe with Co–Ti leads to a decrease of the magnetocrystalline anisotropy (Kojima 1982). This results in a strong decrease of the coercivity and the relative remanence (= remanent magnetization/saturation magnetization) at $x \approx 1.0$ caused by the transition from uniaxial to planar anisotropy. Replacing Fe with Co–Ti leads also to smaller particle sizes. Ti has an effect as a nucleation agent.

For the preparation of nanocrystalline particles ($x = 0.8$) glass flakes from the system $40BaO–33B_2O_3–27(Fe_2O_3 + CoO + TiO_2)$ (in mol%) were heat treated between 570 and 620 °C for long times (hours to days). The samples annealed at 570–600 °C are nearly superparamagnetic. At 580 °C the mean particle size is ≈10 nm. Increasing annealing temperatures lead to an enhanced particle yield and an increasing relative remanence and coercivity due to particle growth. The aspect ratio diameter/thickness of the hexagonal particles increases with increasing particle size up to an almost constant value of about 5–10 depending on the degree of substitution. For similar annealing conditions, higher values of x cause smaller aspect ratios (Görnert *et al* 1990, Pfeiffer *et al* 1993). The magnetic properties are influenced by the decrease of the magnetocrystalline anisotropy caused by CoTi substitution (independent of the size) and have superparamagnetism superimposed due to the small particle size. Particles in the range for such properties were prepared with substitution degrees of 0.95, 1.1, 1.2 and 1.5 by an annealing of 650 °C/4 h.

2.2. Investigations of particle size dependent properties

The experimentally observed size dependences of the specific magnetization of $BaFe_{12}O_{19}$ nanoparticles do not agree with theoretical predictions. One common hypothesis is that a magnetically 'dead' layer is formed at the particle surface, as derived from the drop of the magnetization with decreasing particle size (Kirusu *et al* 1987). For a magnetically 'dead' layer at the particle surface, several explanations are offered: one explanation is the structural transition of the γ-Fe_2O_3 structural subunits of the $BaFe_{12}O_{19}$ matrix to an antiferromagnetic α-Fe_2O_3 phase (e.g. An *et al* 2002) in connection with a decomposition of the $BaO{\cdot}6Fe_2O_3$ type. On the other hand, defects, local disorder and the asymmetric environment play a more important role at the particle surface. In addition, it is reported that a variation of magnetic properties as a function of surface coordination occurs (e.g. Hormes *et al* 2005).

Small angle neutron scattering (SANS) on deuterated ferrofluids, however, gave no clear indication of a magnetic 'dead' layer (Hoell *et al* 2002, 2003). The deuteration of the carrier fluid causes scattering contrast between the surfactant and the carrier fluid. Measurements in an applied magnetic field give a magnetic contrast. The scattering length density inside the particles was constant. The magnetic size investigations fit better to homogeneous particles with reduced magnetization than to particles with a magnetic dead layer and full core magnetization (see figure 1). The magnetic core size distribution was reconstructed from magnetization data under the assumption of a log-normal size distribution (Chantrell *et al* 1978).

The normalized distributions are plotted in figure 1 (curves (a) and (c)) for a FF prepared from a Ba ferrite nanopowder with a mean size of ≈9 nm (from TEM).

Further investigations on this problem were carried out in cooperation with Modrow and Palina (University of Bonn) by spectroscopic methods. In contrast to the SANS results, there is an indication of some surface segregation from photoemission spectra of the Ba LIII XANES

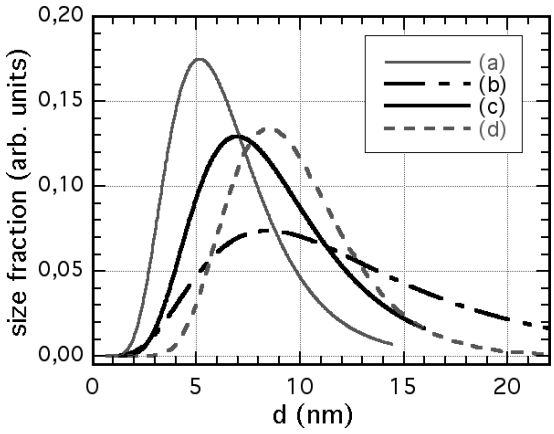

Figure 1. Relative volume size distributions of two ferrofluids (FF) calculated assuming a magnetization of particles equal to (a) the theoretical bulk magnetization, FF from 9 nm particles, (b) the measured magnetization of the powder, FF from 13 nm particles, and (c) the magnetization measured for the powder, FF from 9 nm particles. Part (d) shows SANS data, FF from 9 nm particles.

(x-ray absorption near edge structure) of (Co–Ti doped) barium hexaferrite samples (Palina *et al* 2006).

A magnetic 'dead' layer, to be consistent with the photoemission results, would be less than 1 nm in thickness. EXAFS (extended x-ray absorption fine structure) study shows clearly that the Ba–Fe coordination is reduced significantly with decreasing particle size.

A decomposition of the ferrite into BaO:γ-Fe_2O_3, maghemite, which can be found as a building block in the structure of $BaFe_{12}O_{19}$, could explain the structural similarity of the XANES spectra of this material and bulk barium hexaferrite, but is not sufficient to lead to the observed variations in magnetic properties. However, the hypothesis that haematite is formed could not be supported.

2.3. Influence of the shape anisotropy and behaviour of the remanent magnetization near the transition from uniaxial to planar anisotropy

The influence of the shape anisotropy of Ba ferrite platelets is weak for magnetically uniaxial particles but may play a role for particles in the transition range from uniaxial to planar crystal anisotropy and was therefore investigated theoretically (Hartmann 2004). Anisotropy constants given in Kreisel *et al* (2001) and magnetization values from Kojima (1982) were used for the calculation. A realistic aspect ratio of 4 was assumed. The influence of the shape increases with decreasing crystal anisotropy (i.e. increasing degree of substitution). In figure 2 energetically preferred positions (easy axes of magnetization) are shown by bigger absolute values. On the left-hand side the distribution of the magnetocrystalline anisotropy density is shown, whereas on the right-hand side the shape anisotropy is also considered. The calculations reveal that uniaxial anisotropy is weakened and planar anisotropy increased by shape anisotropy.

In the case of planar crystal anisotropy the in-plane shape anisotropy (in the ab plane) is small and can be neglected. A turning of the magnetization out of the ab plane is possible only at strong fields above the anisotropy field (Klupsch 1989).

For different applications like as magnetic markers for detection in zero field or application of magnetic loss, particles with a high remanent magnetization are required. Usually the magnetic field amplitude is limited; i.e., values at lower fields are important. Experiments

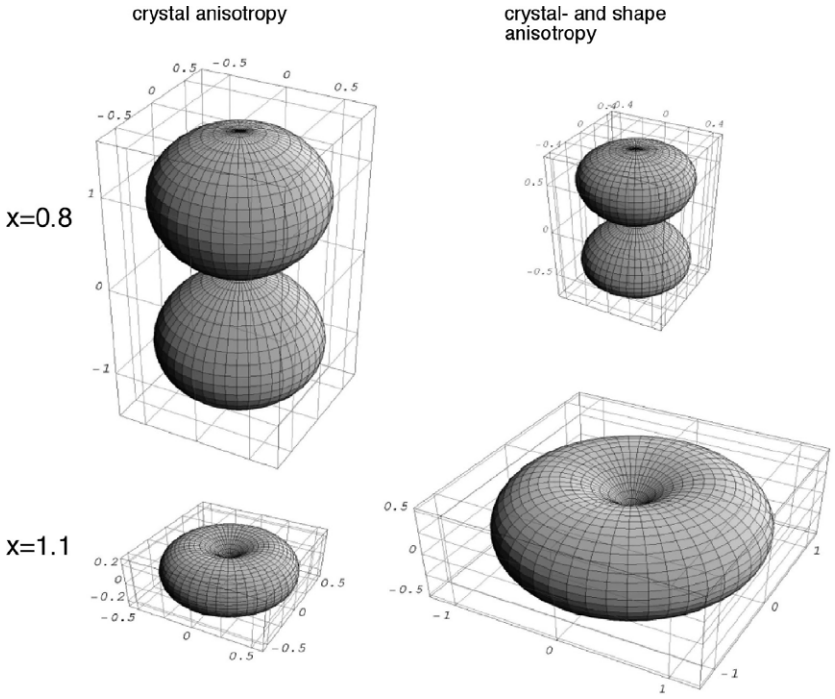

Figure 2. Distribution of the anisotropy energy density for particles with degrees of substitution $x = 0.8$ (uniaxial anisotropy) and $x = 1.1$ (planar anisotropy); the c axis of the particles is vertical; values are in units of 10^5 erg g^{-1}. Left-hand side: magnetocrystalline anisotropy; right-hand side: magnetocrystalline and shape anisotropy.

with barium ferrite samples with different coercivities revealed that powders with $H_C > \approx 12$ kA m^{-1} could not be dispersed even for a short time but form a sediment within minutes. Additionally such particles in suspensions or ferrofluids should therefore show a coercivity as low as possible. Small particles are desirable to avoid sedimentation of the particles.

Static magnetic properties were measured using a vibrating sample magnetometer (VSM), MicroMag^{TM} (Princeton Measurement Corp.). The remanent magnetization of Ba ferrite powders was taken from VSM hysteresis loops. The particles were fixed to exclude Brownian relaxation. Our powders (mean sizes < 30 nm) contain superparamagnetic fractions as well. They show Néel relaxation.

In figure 3 the dependence of the remanent magnetization on the maximum magnetic field of the hysteresis loops can be seen for different degrees of CoTi substitution. The mean particle size is comparable: 16–18 nm calculated from values of the specific surface assuming spherical shape. Particles of magnetically 'softer' ferrites (with a higher degree of substitution) reveal at lower applied fields (some 10 kA m^{-1}) higher remanence values than magnetically harder ferrites at the same low fields. A similar behaviour of the hysteresis losses was found for bigger particles as well as particles from W-type hexaferrite (Müller *et al* 2003). Beside this, only in case of magnetically 'softer' ferrites were loss values close to the maximum (saturation) losses reached at lower fields.

The powder with $x = 1.2$ shows the highest remanence values in the field range relevant for applications. After Smit and Wijn (1959), here the anisotropy (exact crystal anisotropy constants, especially $K_1 + 2K_2$, which is responsible for the planar anisotropy) is smaller than

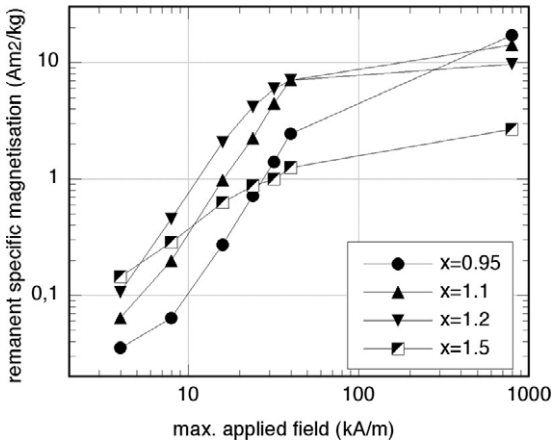

Figure 3. Remanent specific magnetization versus maximum applied field for ferrite nanoparticles with different degrees x of CoTi substitution.

at $x = 1.5$. For definitions of anisotropy constants in different crystal systems see Smit and Wijn (1959).

3. Magnetic iron oxide particles obtained by glass crystallization

3.1. Preparation and structural properties

There have been several investigations into the formation of magnetite particles in non-soluble silicate glasses (e.g. Lembke *et al* 1999). For hyperthermia applications even glass ceramics with zinc ferrite (Kawashita *et al* 2004) or α-Fe (obtained by reduction of iron oxide) (Konaka *et al* 1997) mostly in $CaSiO_3$ matrices were considered. However for advanced kinds of particle applications in cancer therapy a powder suspension is necessary. The preparation of magnetic iron oxide powder by crystallization from $CaO–Fe_2O_3–B_2O_3$ glass and subsequent dissolving of the matrix was demonstrated in Müller *et al* (2004). The preparation of initial glass ceramics containing only Fe_3O_4 or γ-Fe_2O_3, rather than non-magnetic iron oxides, proved to be difficult because a Fe^{2+}/Fe^{3+} ratio high enough to form only Fe_3O_4 ($Fe^{2+}Fe_2^{3+}O_4$) can hardly be achieved. From our experience, even for the preparation of γ-Fe_2O_3 which contains only Fe^{3+} a certain amount of Fe^{2+} is necessary for the phase formation. The fraction of Fe^{2+} from the total iron content is low and increases with higher temperatures. In Ba containing borate glasses a typical value is only 6% at 1250 °C (Tanaka *et al* 1991). The transition from metastable γ-Fe_2O_3 to the stable non-magnetic α-Fe_2O_3 has to be avoided as well.

The glass flakes were annealed at temperatures of 500–700 °C for several hours to days. In a first series of samples with a single-step annealing the annealed flakes show a specific saturation magnetization which corresponds to a yield of ≈70% of Fe_3O_4 (estimated from magnetization data assuming bulk magnetization). The formation of a second magnetic phase ε-Fe_2O_3 (Müller *et al* 2004) could be avoided through improved melting and quenching conditions. Maximum specific magnetization values of 64 $A\,m^2\,kg^{-1}$ were reached for the powders.

Investigations using x-ray diffraction (XRD; Xpert, Philips) show that in the flake samples there is a mixture of Fe_3O_4 (JCPDS No 19-0692) and γ-Fe_2O_3 (JCPDS No 39-1346) in a CaB_2O_4 matrix. In comparison, XRD peaks of separated iron oxide powders shift in most cases

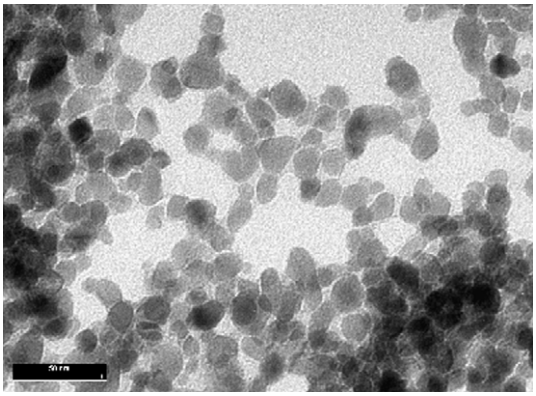

Figure 4. TEM image of a dried maghemite ferrofluid (bar: 50 nm). (Reprinted from Müller *et al* (2005), Copyright 2005, with permission from Elsevier.)

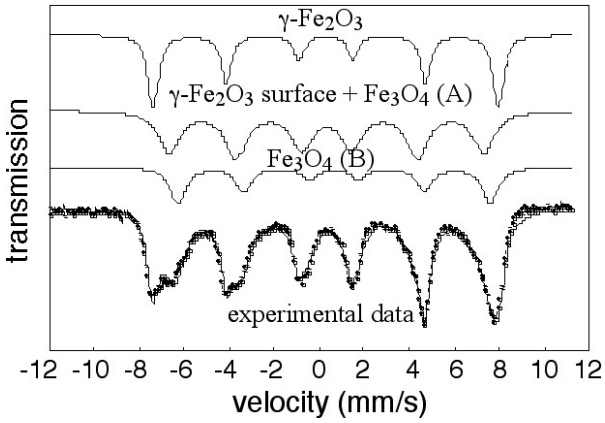

Figure 5. Room temperature Mössbauer spectra of an iron oxide containing glass, annealed at 640 °C.

toward γ-Fe_2O_3 ones, as was confirmed by Mössbauer spectroscopy by R Zboril (University of Olomouc, Czech Republic).

A water based charge stabilized ferrofluid was prepared from particles (specific magnetization: 62.8 A m^2 kg^{-1}; coercivity: 1.03 kA m^{-1}) of the flake sample in connection with the dissolving of the borate by acetic acid. Surfactants were not used. The number of aggregates in the fluid was reduced by centrifugation, which may result in a change of the size distribution between particles in the flakes and in the fluid. After rinsing, the fluid is weakly acidic.

The mean particle size in the glass sample determined using XRD was 10 nm, whereas a size of 13 nm may be estimated from a TEM image (figure 4) of a dried ferrofluid sample. The particle shape deviates from spherical. From magnetization data we calculated the mean diameter D and the deviation σ of the log-normal size distribution according to Chantrell *et al* (1978) and obtained $D = 11.3$ nm and $\sigma = 0.51$ for the fluid sample. The Mössbauer measurements did not show a superparamagnetic fraction in the glass sample with 11 nm particles (see figure 5). Differences from VSM measurements can be explained by the different

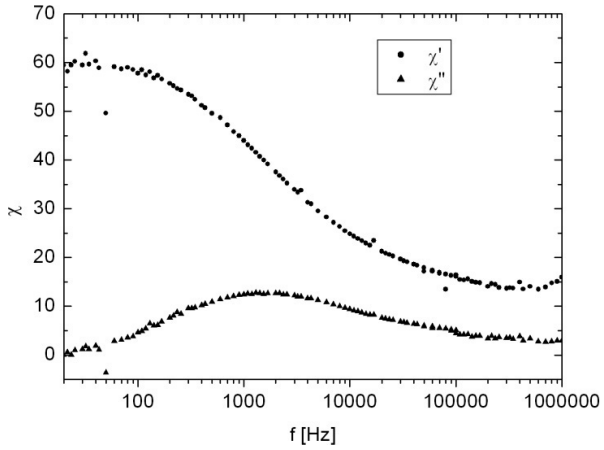

Figure 6. Spectra of the complex susceptibility of a fluid from 13 nm particles. (Reprinted from Müller *et al* (2005), Copyright 2005, with permission from Elsevier.)

fractions of superparamagnetic particles depending on the time constants of the measurement methods.

In a second series of samples the influences of separate steps for nucleation and particle growth during heat treatments of flakes (in Ar atmosphere) were investigated. The annealed flakes show a high specific saturation magnetization that corresponds to a yield up to ≈78% of Fe_3O_4. The separated powders show magnetization values up to 70 A m^2 kg^{-1} close to literature values for γ-Fe_2O_3. There was no haematite found from the XRD. The mean particle size was about 16 nm.

3.2. Magnetic properties

Magnetic losses of particles in a fluid sample were investigated via measurements of ac susceptibility spectra, hysteresis loops as well as direct calorimetry. The particles are separated from a glass annealed at 640 °C (single step). The preparation of the fluid is described in Müller *et al* (2005). The results are compared for a field amplitude of 11 kA m^{-1} and a frequency of 410 kHz which proved highly suitable for hyperthermia in animal experiments (Hilger *et al* 2001).

Results of ac susceptibility measurements are shown in figure 6. From the imaginary part, which clearly shows a peak which has to be ascribed to Brown relaxation (Hergt *et al* 2004b), one may extrapolate a specific loss power of 160 W g^{-1} for the field parameters mentioned above.

For comparison with results from ac susceptibility, hysteresis losses were determined by integration of the hysteresis minor loop area. SLP values of 16, 8 and 30 W g^{-1} result for particles in glass flakes, powder and immobilized fluid taking again the above mentioned field parameters. Considering the different values of 160 and 30 W g^{-1} one has to keep in mind that hysteresis and Néel losses are due to different mechanisms which are representative for particles having different core diameters within the size distribution of one sample.

In order to get a direct measure of magnetic losses being converted into heat, calorimetric loss measurements relevant for applications were performed by measuring the increase of temperature of a sample in a coil which generates an ac magnetic field of 11 kA m^{-1} at a frequency of 410 kHz. The results are 20, 8.9 and 87 W g^{-1} for flakes, powder and the immobilized fluid mentioned above.

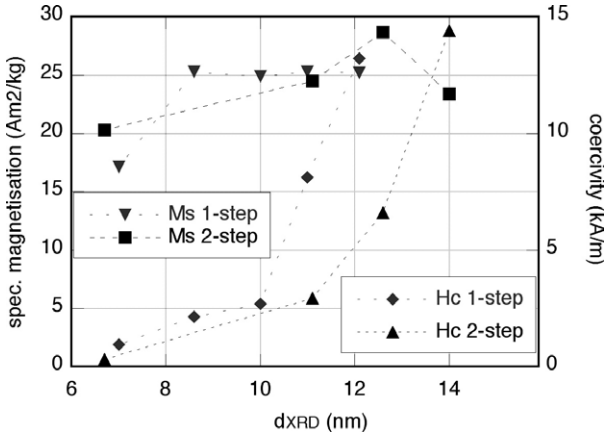

Figure 7. Specific magnetization and coercivity versus the mean particle size by XRD for glasses containing iron oxide particles after a one-step and after a two-step annealing, respectively.

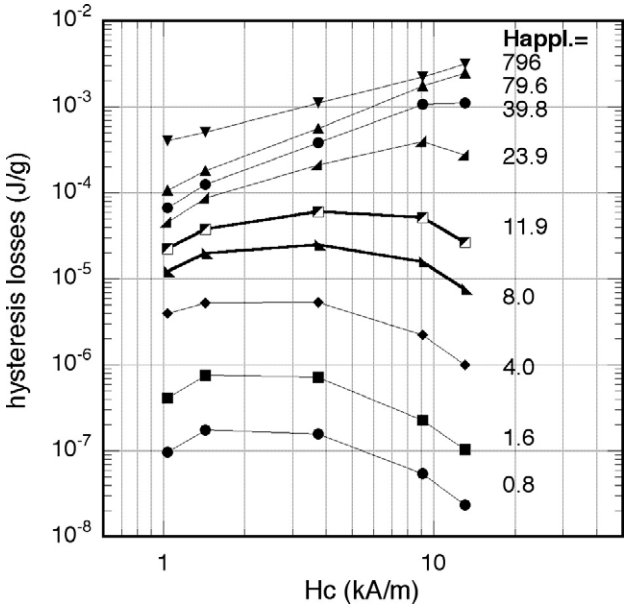

Figure 8. Dependence of the hysteresis losses at a certain maximum applied fields H_{appl} on the coercivity (of saturation magnetization loops) of powder samples.

The two-step annealing flake samples show smaller coercivities at comparable mean particle sizes in the superparamagnetism–ferrimagnetism transition range (figure 7) than samples after a one-step annealing. Therefore the fraction of particles giving maximum hysteresis losses at a small field amplitude is larger and the specific hysteresis losses at comparable coercivity of the samples are higher than for samples after a one-step annealing. A hysteresis loss power of 21 W g^{-1} could be determined for a powder and 43 W g^{-1} for a ferrofluid prepared from such a powder.

Figure 8 demonstrates the dependence of the hysteresis losses achieved at a certain maximum applied field H_{appl} on the coercivity (of saturation magnetization loops) of the

powder samples. As expected, in order to obtain the maximum losses at a certain maximum applied field, with increasing coercivity of the samples, higher applied fields are necessary. For heating applications using a field of 11 kA m^{-1} the optimum coercivity is about 4 kA m^{-1}. This result is in reasonable agreement with conclusions (Andrä 2005) derived from the Stoner–Wohlfarth theory (Stoner and Wohlfarth 1948).

3.3. Coating experiments in connection with the dissolving of the matrix

To obtain the particles the matrix is dissolved using a weak diluted acid, usually acetic acid. Acetic acid enables the preparation of charge stabilized ferrofluids but for an effective steric repulsion of the particles the chain length is too small. Besides the usual separation of the particles from the matrix achieved by dissolving the matrix with diluted acetic acid, some experiments were done with citric acid and glycolic acid.

Citric acid is known as one possible particle coating material for some aqueous charge stabilized ferrofluids with small superparamagnetic particles. The aim was to add the coating material at the very beginning of the dissolving process in contrast to the usual procedure where the coating material or surfactant is added after removing the acetic acid and rinsing the ferrofluid.

Dissolving the matrix by means of citric acid leads to partly dissolving the iron oxide particles. The effect can be seen clearly even in the case of diluted 2% citric acid through a greenish colour of the solution. Another problem is the formation of weakly soluble calcium citrate tetrahydrate which has not led to stable particle suspensions up to now.

Encouraging experiments with glycolic acid were carried out by Schmidt (University of Düsseldorf, Germany). The aim was a particle surface modification for a polymerization of a biocompatible coating by means of the second functional group of the glycolic acid. The synthesis is performed on glass flakes, that are treated with 1.4 mass% glycolic acid (aqueous) to dissolve the matrix and to functionalize the particle surface by chemisorption of the acid. In this way, hydroxy groups are immobilized on the surface and may act as initiating species in the following surface-initiated polymerization of ε-caprolactone. Traces of water are removed by washing cycles and aceotropic distillation. Afterwards, the particles are transferred to ε-caprolactone monomer, Sn(II) octoate is added as a catalyst and the mixture is heated to 130 °C for 5 h. After cooling it to 80 °C, toluene is added to yield a dispersion of poly(ε-caprolactone)-coated maghemite nanoparticles in toluene. The concentration of the ferrofluid on maghemite obtained is about 1.0 mass%. The specific hysteresis loss powers of the dried powder and the fluid are 11 and 46 W g^{-1}, respectively, at the usual field parameters.

4. Precipitated iron oxide particles obtained by cyclic growth

4.1. Preparation and structure of the particles

To influence and improve the mean size as well as the size distribution of magnetic iron oxide nanoparticles a second preparation method is promising where further growth of the particles is possible on small given particles without further nucleation. This approach was demonstrated for a non-aqueous system by Klokkenburg *et al* (2004).

Nanocrystalline magnetic iron oxide particles for ferrofluids are usually prepared by wet chemical precipitation (Khallafalla and Reimers 1980, Massart 1981) from aqueous iron salt solutions by means of an alkaline solution like KOH or NH_4OH, according to $Fe^{2+} + 2Fe^{3+} + 8OH^- \rightarrow Fe_3O_4 + 4H_2O$. Numerous publications describe variations of this preparation method using different iron salts and alkaline solutions. Typical particle sizes are in the region of 10 nm. To influence the mean particle size in the range >15 nm and

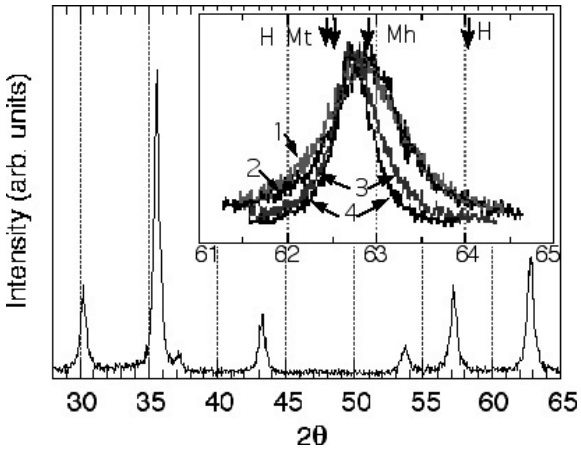

Figure 9. The XRD pattern (Cu Kα) shows spinel structure. The inset shows the 440 peak of samples from different numbers of cycles. The arrows indicate the theoretical peak positions for magnetite (M_t), maghemite (M_h) and haematite (H; 214 and 300 peaks). (Müller *et al* (2006); with permission from ©2006 Oldenbourg Wissenschaftsverlag GmbH.)

especially the size distribution is difficult and hardly possible, respectively, by the usual wet precipitation method. By modification of the precipitation parameters, for instance temperature or concentration, obtaining bigger particles (≈20 nm) is possible, but they show a wide size distribution (Goetze *et al* 2002).

We prepared our particles by growth, cycle by cycle, on initial particles which were prepared by the 'usual' method mentioned above (Müller *et al* 2006). A 1 M $NaHCO_3$ solution was slowly added to a $FeCl_2/FeCl_3$ solution (Fe^{2+}–Fe^{3+}-ratio = 1:1) under permanent stirring up to pH = 7 which led to the formation of a brownish precipitate. Then a new Fe^{2+}/Fe^{3+} mixture was added at the same amount, like in the first cycle, and the precipitation was carried out again. This procedure was repeated three or four times. After that the solution was boiled for 10 min to form an almost black precipitate. The magnetic nanoparticles were then washed with water and dried. For investigations of the progress of growth, a small sample of particles was taken after each cycle, boiled and washed as well. Some coating experiments were carried out with iron oxide particles (before drying) prepared by a modified wet precipitation method with one cycle to simplify the experiment. Usual particle sizes here are about 16 nm.

X-ray diffraction investigations were carried out to determine the phase content of the powder samples and the mean particle size from line broadening of the 440 peak using the Scherrer equation, assuming there is no contribution of strain to the broadening. Investigations via XRD show spinel iron oxide as the only phase (see figure 9). With increasing number of cycles a narrower linewidth and a small shift of the peak position to lower 2θ angles can be observed (figure 9, inset). Despite the Fe^{2+} excess in the initial materials compared to $Fe^{2+}Fe_2^{3+}O_4$, in the bigger particles (three and four cycles) there is a mixture of Fe_3O_4 (JCPDS No 19-0692) and γ-Fe_2O_3 (JCPDS No 39-1346), whereas the peak positions for smaller particles (one or two cycles) indicate mostly γ-Fe_2O_3. The formation of haematite (α-Fe_2O_3) could be avoided. The mean particle sizes of the series considered are 10, 11, 21 and 26 nm, respectively.

4.2. Magnetic properties

In the following the development of the magnetic properties of powder samples with increasing number of cycles (i.e. particle size) is described (figure 10). The specific saturation

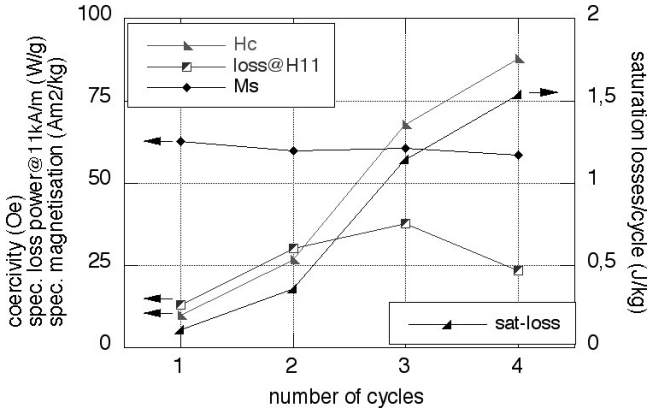

Figure 10. Magnetic properties depending on the number of cycles. (Müller *et al* (2006); with permission from ©2006 Oldenbourg Wissenschaftsverlag GmbH.)

Table 1. Properties of comparable samples prepared with one and three cycles.

Cycles	D_{XRD} (nm)	Coercivity (kA m^{-1})	Magnetization (A m^2 kg^{-1})	SLP (W g^{-1})
1	14.3	**3.7**	65.6	27
3	**16.8**	**3.7**	67.7	35
1	**16.6**	5.65	73.2	22

magnetization remains almost constant, as expected. The coercivity and the parallel hysteresis losses at saturation field increase strongly. However the hysteresis losses at low field (11 kA m^{-1}) reveal a maximum at the third cycle (21 nm). The particles after the fourth cycle with 26 nm mean particle size are probably already magnetically too hard (H_C = 7.0 kA m^{-1}) to give optimal losses at the low applied field. Hard magnetic particles should be avoided as well because of enhancement problems as regards the preparation of a stable particle suspension.

The samples prepared by cycles have to be compared with samples obtained by a modified 'usual' wet chemical method with one cycle (table 1). The specific loss power (SLP) was calculated from hysteresis loops for 410 kHz and 11 kA m^{-1}. The three-cycle sample shows at comparable mean size D_{XRD} (bold numbers) a smaller coercivity (or has at comparable coercivities (bold numbers) a bigger mean size) and therefore a higher hysteresis loss power at low magnetic field. Former measurements of zero-field cooled magnetization curves (ZFC; the dependence on T of the magnetization in a weak magnetic field) may suggest a narrower distribution of blocking temperatures in the case of the three-cycle sample compared with the one-cycle sample with similar mean size (Müller *et al* 2006).

In order to consider all the loss mechanisms, again calorimetric measurements on the three-cycle sample were carried out at 400 kHz and field amplitudes of 11.5 and 24.5 kA m^{-1}. The resulting specific loss powers are 81 and 314 W g^{-1}, respectively. Figure 11 shows the hysteresis losses per cycle and calorimetric losses (divided by the frequency) of the three-cycle sample, and the hysteresis losses of the one-cycle/14.3 nm sample with the same coercivity (see table 1). For comparison, losses of magnetosomes, being the highest known up to now (Hergt *et al* 2005), and losses of a commercial powder (mean size from XRD: 30 nm) are given. The two samples have similar mean particle sizes but differ in their size distributions: very narrow in the case of magnetosomes and very wide for the commercial powder.

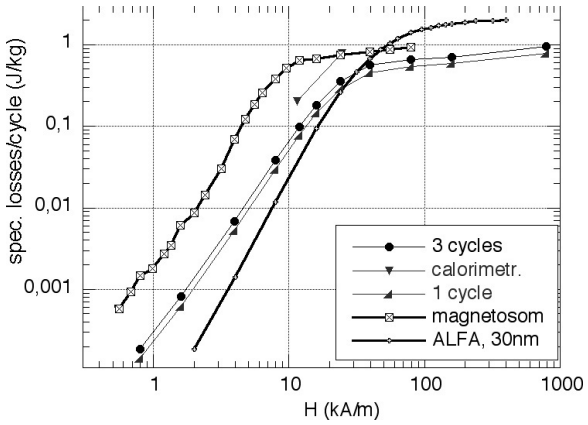

Figure 11. Specific hysteresis losses depending on the magnetic field amplitude. (Müller *et al* (2006); with permission from ©2006 Oldenbourg Wissenschaftsverlag GmbH.)

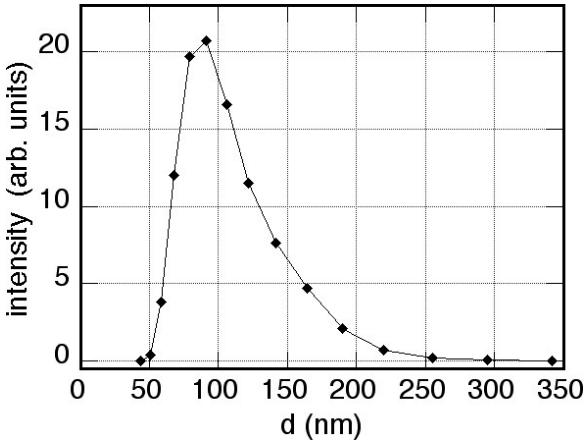

Figure 12. Number distribution of the hydrodynamic diameter of a ferrofluid from CMD-coated particles obtained by dynamic light scattering.

4.3. Coating experiments and properties of magnetic fluids

For medical *in vivo* applications of iron oxide nanoparticles a biocompatible coating is necessary. One coating material used is carboxymethyl dextran (CMD) suitable for the covalent fixation of bioactive molecules. Our initial material was CMD sodium salt from Fluka.

Typically, the nanoparticle dispersion was separated magnetically and washed three times with water. After addition of water and adjusting the pH with diluted HCl to 3–4, the suspension was warmed to 45 °C and an aqueous solution of CMD was added. The mixture was homogenized by ultrasonic treatment for 1 min using a Sonopuls GM200 (Bandelin) device. The suspension was stirred for a further 60 min at 45 °C and the coated nanoparticles were separated magnetically and washed once with water.

The ferrofluids prepared from particles smaller than about 17 nm (from XRD) are stable as regards sedimentation. Figure 12 shows the number distribution of the hydrodynamic diameters measured by means of dynamic light scattering (DLS; HPP5001, Malvern Instruments) by Gelbrich (University of Düsseldorf, Germany). The primary iron oxide particle size of this

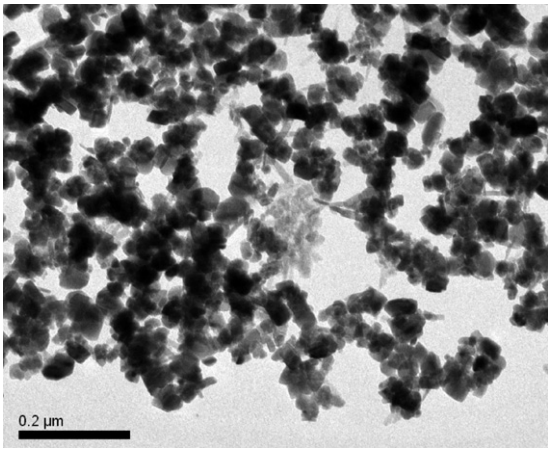

Figure 13. TEM image of particles of a dried ferrofluid prepared in three growth cycles.

sample is 16.3 nm, from XRD. The coercivity of the immobilized ferrofluid is 3.8 kA m^{-1}. In contrast, fluids from particles larger than about 17 nm already show a partial sedimentation after just a short time.

Mean particle sizes obtained by means of XRD measured for one sample with bigger iron oxide particles taken from the sediment and from the stable supernatant after one day are 17.4 and 21 nm, respectively. The particles were prepared by a three-cycle procedure. The mean value of the original sample was 19.3 nm. In figure 13(a) a TEM image of the dried original fluid after re-dispersing by shaking is given. The particles in the figure had been magnetized before and during the washing step of the preparation which may influence the agglomerate structure. The coercivity of the immobilized ferrofluid is 4.1 kA m^{-1}. Typical dried fluid samples show a mass loss (mainly at about 220 °C) according to thermogravimetry (Netzsch STA409) of about 6% which can be interpreted as the amount of CMD on the particle surface.

After about two weeks a considerable agglomeration could be observed in all samples, which probably results from an ageing effect of the CMD layer.

5. Summary

Summarizing the results, the glass crystallization method as well as a method of cyclic growth from aqueous solution was successfully used in order to prepare magnetic iron oxide nanoparticles with increased mean particle sizes. With both methods, the particle size distribution can be influenced. The biggest particles are already magnetically too hard to give a high specific loss power SLP at low magnetic field amplitudes. Good SLP values found were of the order of 100 W g^{-1} at 400 kHz and 11 kA m^{-1}, which is sufficient for tumour therapy by intratumoural injection but not for advanced kinds of particle applications in the future like tumour antibody targeting. Therefore a further particle optimization with respect to mean size and size distribution width is necessary.

The glass crystallization method is suitable also for preparing Ba ferrite particles with a mean size and intrinsic anisotropy which are suitable for the preparation of magnetic fluids.

Acknowledgments

The authors thank Dr H Modrow and Dr N Palina (University of Bonn, Germany) for XANES/EXAFS investigations, Dr R Zboril (University of Olomouc, Czech Republic) for

Mössbauer investigations and Dr A Schmidt and T Gelbrich (University of Düsseldorf, Germany) for coating experiments and DLS measurements, respectively.

We thank H Steinmetz, C Schmidt, Ch Schmidt and A Steinbrück for support.

The present work was supported by the Deutsche Forschungsgemeinschaft in the framework of SPP1104 under contracts Nos Ga662/3-1 and He2878/9-2.

References

An S Y, Lee S W and Kim C S 2002 Magnetic properties of $Ba_{1-x}Sr_xFe_{12}O_{19}$ grown by a sol–gel method *J. Magn. Magn. Mater.* **242** 413–5

Andrä W 2005 private communication

Brückl H, Brzeska M, Brinkmann D, Schotter J, Reiss G, Schepper W, Kamp P B and Becker A 2004 Magnetoresistive logic and biochip *J. Magn. Magn. Mater.* **282** 219–24

Chantrell R, Popplewell J and Charles S W 1978 Measurements of particle size distribution parameters in ferrofluids *IEEE Trans. Magn.* **14** 975

Chen H S and Miller C E 1970 A rapid quenching technique for the preparation of thin uniform films of amorphous solids *Rev. Sci. Instrum.* **41** 1237–8

Goetze T, Gansau C, Buske N, Roeder M, Görnert P and Bahr M 2002 Biocompatible magnetic core/shell nanoparticles *J. Magn. Magn. Mater.* **252** 399–402

Görnert P, Sinn E and Rösler M 1990 Barium ferrites for magnetic recording media *Mater. Sci. Forum* **62–64** 573–6

Görnert P, Sinn E and Rösler M 1991 Preparation and characterization of hexaferrite powders *Key Eng. Mater.* **58** 129–48

Hartmann C 2004 Herstellung und Charakterisierung von dotierten nanokristallinen Barium-hexaferritpartikeln im Übergangsgebiet von uniaxialer zu planarer Anisotropie *Diploma Thesis* FH Jena/IPHT

Hergt R, Andrä W, d'Ambly C G, Hilger I, Kaiser W A, Richter U and Schmidt H G 1998 Physical limits of hyperthermia using magnetite fine particles *IEEE Trans. Magn.* **34** 3745–54

Hergt R, Hiergeist R, Hilger I and Kaiser W A 2002 Magnetic nanoparticles for thermoablation *Recent Res. Dev. Mater. Sci.* **3** 723–42

Hergt R, Hiergeist R, Zeisberger M, Glöckl G, Weitschies W, Ramirez L P, Hilger I and Kaiser W A 2004a Enhancement of AC-losses of magnetic nanoparticles for heating applications *J. Magn. Magn. Mater.* **280** 358–68

Hergt R, Hiergeist R, Hilger I, Kaiser W A, Lapatnikov Y, Margel S and Richter U 2004b Maghemite nanoparticles with very high AC-losses for application in RF-magnetic hyperthermia *J. Magn. Magn. Mater.* **270** 345–57

Hergt R, Hiergeist R, Zeisberger M, Schüler D, Heyen U, Hilger I and Kaiser W A 2005 Magnetic properties of bacterial magnetosomes as potential diagnostic and therapeutic tools *J. Magn. Magn. Mater.* **293** 80–6

Hilger I, Andrä W, Hergt R, Hiergeist R, Schubert H and Kaiser W A 2001 Electromagnetic heating of breast tumors in interventional radiology *in vitro* and *in vivo* studies in human cadavers and mice *Radiology* **218** 570–5

Hoell A, Müller R, Wiedenmann A and Gawalek W 2002 Core–shell and magnetic structure of barium hexaferrite fluids studied by SANS *J. Magn. Magn. Mater.* **252** 92–3

Hoell A, Müller R, Heinemann A and Wiedenmann A 2003 Structure investigations of barium-hexaferrite ferrofluids and its precursors by SANS with polarized neutrons *Magnetohydrodynamics* **39/1** 109–16

Hormes J, Modrow H, Bönnemann H and Kumar C S S R 2005 The influence of various coatings on the electronic, magnetic, and geometric properties of cobalt nanoparticles *J. Appl. Phys.* **97** 10R102

Kawashita M, Iwahashi Y, Kokubo T, Yao T, Hamada S and Shinjo T 2004 Preparation of glass-ceramics containing ferrimagnetic zinc–iron ferrite for the hyperthermal treatment of cancer *J. Ceram. Soc. Japan* **112** 373–9

Khallafalla S E and Reimers G W 1980 Preparation of dilution-stable aqueous magnetic fluids *IEEE Trans. Magn.* **16/2** 178–83

Kirusu S, Ido T and Yokoyama H 1987 Surface effect on saturation magnetization of Co and Ti substituted Ba-ferrite fine particles *IEEE Trans. Magn.* **23** 3137–9

Klokkenburg M, Vonk Ch, Claesson E M, Meeldijk J D, Erné B H and Philipse A P 2004 Direct imaging of zero-field dipolar structures in colloidal dispersions of synthetic magnetite *J. Am. Chem. Soc.* **126** 16706–7

Klupsch T 1989 Magnetization curve and magnetic characterization of a system of fine single domain particles with oblate ellipsoidal shape and planar magnetocrystalline anisotropy *Phys. Status Solidi* **113** 561–72

Kojima H 1982 Fundamental properties of hexagonal ferrites with magnetoplumbite structure *Ferromagnetic Materials* vol 3, ed E P Wohlfarth (Amsterdam: North-Holland) pp 305–93

Konaka H, Miyaji F and Kokubo T 1997 Preparation and magnetic properties of glass-ceramics containing a-Fe for hyperthermia *J. Ceram. Soc. Japan* **105** 894–8

Kreisel J, Vincent H, Tasset F, Pate M and Ganne J P 2001 An investigation of the magnetic anisotropy change in $BaFe_{12-2x}Ti_xCo_xO_{19}$ single crystals *J. Magn. Magn. Mater.* **224** 17–29

Lembke U, Hoell A, Kranold R, Müller R, Schüppel W, Goerigk G, Gilles R and Wiedenmann A 1999 Formation of magnetic nanocrystals in a glass ceramic studied by small-angle scattering *J. Appl. Phys.* **85/4** 2279–85

Massart R 1981 Preparation of aqueous magnetic liquids in alkaline and acidic media *IEEE Trans. Magn.* **17/2** 1247–8

Müller R, Hergt R, Zeisberger M and Gawalek W 2005 Preparation of magnetic nanoparticles with large specific loss power for heating applications *J. Magn. Magn. Mater.* **289** 13–6

Müller R, Hiergeist R, Gawalek W and Hoell A 2003 Ba-ferrite particles for magnetic liquids with enhanced Néel relaxation time and loss investigations *Magnetohydrodynamics* **39/1** 47–50

Müller R, Steinmetz H, Hiergeist R and Gawalek W 2004 Magnetic particles for medical applications by glass crystallisation *J. Magn. Magn. Mater.* **272–276** 1539–41

Müller R, Steinmetz H, Zeisberger M, Schmidt Ch, Dutz S, Hergt R and Gawalek W 2006 Precipitated iron oxide particles by cyclic growth *Z. Phys. Chem.* **220** 51–7

Palina N, Modrow H, Müller R, Hormes J, Dowben P A and Losovyj Ya B 2006 The electronic structure and band hybridization of Co/Ti doped $BaFe_{12}O_{19}$ *Mater. Lett.* **60** 236–40

Pfeiffer H, Chantrell R W, Görnert P, Schüppel W, Sinn E and Rösler M 1993 Properties of barium hexaferrite powders for magnetic recording *J. Magn. Magn. Mater.* **125** 373–6

Shirk B T and Buessem W R 1970 Magnetic properties of barium ferrite formed by crystallization of a glass *J. Am. Ceram. Soc.* **53** 192–6

Smit J and Wijn H P J 1959 *Ferrites* (Eindhoven: Philips Technical Library) p 208

Stoner E C and Wohlfarth E P 1948 A mechanism of magnetic hysteresis in heterogeneous alloys *Phil. Trans. R. Soc.* A **240** 599–642

Tanaka K, Kamiya K, Yoko T, Tanabe S, Hirao K and Soga N 1991 Electron spin resonance study of iron ion clusters in borate glasses *Phys. Chem. Glasses* **32/1** 16–21